Construction and Building Materials 94 (2015) 323–336

Contents lists available at ScienceDirect

Construction and Building Materials

journal homepage: www.elsevier.com/locate/conbuildmat

Evaluation of cement-treated mixtures with slow setting bitumen emulsion as base course material for road pavements

Mojtaba Shojaei Baghini [a,b,*], Amiruddin Ismail [a,b], Mohamed Rehan Bin Karim [c]

[a] Sustainable Urban Transport Research Centre (SUTRA), Universiti Kebangsaan Malaysia, Malaysia
[b] Department of Civil and Structural Engineering, Universiti Kebangsaan Malaysia, Malaysia
[c] Department of Civil Engineering, Faculty of Engineering, University of Malaya, Malaysia

HIGHLIGHTS

- The long-term performance of CBETB was investigated.
- The use of 4% C–3% BE in the pavement base layer are recommended.
- WD tests on 4% C–3% BE mix resulted in a weight losses of 211.95%.
- Additive remarkably improved the permanent deformation of CBETB.
- Zhou three-stage model was developed for DC and WT of CBETB.

ARTICLE INFO

Article history:
Received 18 January 2015
Received in revised form 25 May 2015
Accepted 12 July 2015
Available online 15 July 2015

Keywords:
Bitumen emulsion
Portland cement
Dynamic creep
Mixture
Water absorption
Model

ABSTRACT

This study investigated the effects of the addition of a bitumen emulsion and Portland cement on the long-term performance of road base. The specimens stabilized with Portland cement (0–6%), bitumen emulsion (0–6%) and Portland cement–bitumen emulsion mixture were subjected to different stress sequences in order to study the unconfined compressive strength (UCS), flexural strength (FS), wetting and drying (WD), soaked and unsoaked California bearing ratio (CBR), dynamic creep (DC), and wheel-tracking (WT) characteristics of 7-day-cured specimens. The results of UCS, FS and CBR tests revealed that the additives significantly improved the strength of the mixture. The WD cycling tests showed that the addition of a 4% Portland cement–3% bitumen emulsion mixture resulted in a 179.4% reduction in water absorption, a volume change of 256.3%, and a weight change of 211.95% as compared to the sample with 4% cement after 12 WD cycles. The permanent strain behavior of the samples was assessed by the Zhou three-stage model. The results of DC and WT tests showed that the permanent deformation characteristics were considerably improved by the addition of a 4% Portland cement–3% bitumen emulsion mixture, which resulted in reduction of permanent strain of the mixture. Therefore, this research presents an environmentally friendly additive with outstanding engineering properties for use in road bases.

1. Introduction

A variety of soils or granular materials are available for the construction of road bases, but they may exhibit inadequate properties, e.g., low bearing capacity, susceptibility to moisture damage, and susceptibility to environmental conditions, which would in turn result in substantial pavement distress and shortening of pavement life. However, the addition of a stabilizing agent can improve the properties of a soil-aggregate mixture. Soil-aggregate stabilizers are categorized as either traditional or nontraditional. Traditional additives include cement, lime, fly ash, and bituminous materials, whereas nontraditional additives include enzymes, liquid polymers, resins, acids, silicates, ions, and lignin derivatives. Among these different stabilizing materials, a cement-treated base (CTB) material has significantly high stiffness and strength and exhibits good serviceability and high durability when used for pavement construction. Cement stabilization of soil was first used on a trial basis in 1917, and since then several works have been published on this topic [1–6]. Recently, heavier lorries with exceeding tyres pressures, heavy traffic loads, environmental effects, and high cost of petroleum-derived materials due

* Corresponding author at: Sustainable Urban Transport Research Centre (SUTRA), Universiti Kebangsaan Malaysia, Malaysia.

E-mail addresses: msbaghini@yahoo.com (M.S. Baghini), aismail@ukm.edu.my (A. Ismail), rehan@um.edu.my (M.R. Bin Karim).

http://dx.doi.org/10.1016/j.conbuildmat.2015.07.057
0950-0618/

to the energy crisis have motivated researchers to develop more cost-effective asphalt pavement treated technologies. In this context, cold-in-place stabilization is one of the most capable technologies for its technical reliability, cost-effectiveness, and low environmental impact. In fact, it was recognized in various studies that in road base treatment applications, bitumen emulsion–cement mix modifications improve aggregate bonding, thermal susceptibility, abrasion resistance, and resistance against bleeding, to provide adequate flexibility or to be utilized as an adhesive material [7–9]. However, the type of bitumen emulsions, the compatibility between bitumen and cement, and the amount of bitumen emulsions to be added to the mixture must be carefully designed. The environmental benefit of asphalt emulsion is particularly positive when used for in-place or on-site techniques that avoid the energy usage and emissions associated with heating, drying, and haulage of aggregate. Emulsified asphalt must revert to a continuous asphalt film in order to act as cement in road materials which inclusive removal of the water (breaking), flocculation and coalescence of the emulsion droplets. The droplets are concentrated; leading to coalescence as water leaves the system. The basic mechanism for breaking slow-setting emulsions can be evaporation and absorption of water by the aggregate. However, the emulsifier absorption onto the surface of aggregate, the emulsion droplets movement to the surface of aggregate, and the chemical reactions (pH change) between the bitumen emulsion and the soil aggregate contribute to the emulsion setting [7,8]. The setting speed and curing procedure depend on the bitumen emulsion reactivity, aggregate reactivity, bitumen viscosity, environmental effects (humidity, wind, temperature, etc.) and mechanical reaction. Less viscous asphalts tend to give faster coalescence. In other words, in order to enable the asphalt binder to properly disperse in the aqueous phase, it is necessary that its viscosity be relatively low. In addition, lower viscosity asphalts coalesce more rapidly than high viscosity asphalts and allowing it to be used at lower temperature in the mixture [7,10]. The strength of the reaction of emulsion with aggregate is in many cases sufficient to squeeze the water from the system. A considerable amount of research has been expended to elucidate the mechanism of setting and curing of asphalt emulsion [7,10]. The relative timescale of flocculation (setting) and coalescence (curing) depends on the system, but in general, flocculation is the more rapid process in which some water can be expelled from the system and some cohesive strength develops, followed by a slower coalescence process, which results in a continuous asphalt phase. This asphalt phase must also adhere to the aggregate. Bitumen emulsion–cement compatibility can be evaluated by the stability of emulsion when blended with cement. The stability of the blended bitumen-emulsion and Portland cement must be evaluated as the bitumen emulsion stability will be affected by the cement hydration consumption of water, pH change caused by the Portland cement, and particle charges in the blend [8,9,11–15]. Water in bitumen emulsion consumes due to cement hydration, which reduces the emulsion spaces between the micelles and increases the incorporation of asphalt micelles. Several researches indicated that cement–bitumen emulsion treated base (CBETB) can provide cost-effective solutions to many common designs and construction situations and provide additional strength and support without increasing the total thickness of the pavement layers [8,16]. In addition, depending on project needs, CBETB increases the construction speed, enhances the structural capacity of the pavement, or in some cases reduce the overall time project. A stiffer base reduces deflections due to heavy traffic loads, thereby extending pavement life [4,17–22]. Moreover, CBETB can distribute loads over a wider area and reducing the stresses on the subgrade. It has a high load-carrying capacity, does not consolidate further under load, reduces rutting in hot mix asphalt pavements, and is resistant to freeze–thaw, wetting–drying deterioration [23–25]. Earlier studies [8,9,26–30] clearly demonstrated various benefits from cement–bitumen emulsion addition. This study has extended in terms of both quantifying performance-based mechanical properties and investigating the effects of variables on CBETM using significant predicting model which is not published earlier. The goals of the present work were:

- To assess the factors affecting the short-term performance and strength of a cement–bitumen emulsion-treated base (CBETB) via laboratory tests aimed at determining its unconfined compressive strength (UCS), flexural strength (FS), and unsoaked California bearing ratio (CBR).
- To investigate the long-term performance of stabilized soil-aggregate specimens by conducting soaked CBR, DC, and WT tests on specimens cured for 7 days; these are the most frequently employed factors for assessing the performance of road base stabilization (RBS).
- To study the durability of CBETB subjected to wetting and drying (WD) cycles. The durability of CBETB can be significantly affected by environmental conditions, which considered to evaluate these effects on the performance of CBETB.
- To determine the optimum content of Portland cement and bitumen emulsion in CBETB.
- To compare the effects of the additives on the mixtures using significant prediction models.

WD cycles can be destructive and damage the construction of RBS. However, there are no previous studies showing the behavior of CBETB subjected to WD cycles and permanent deformation of the pavement structure. Hence, it is important to study the effect of environmental conditions and evaluate the permanent strain potential of CBETB.

2. Standard requirements for use of graded soil-aggregate in bases of highways

Quality-controlled graded aggregates are expected to provide appropriate stability and load support for highway and airport bases or sub-bases. This requirement delineates the aggregate size, variety, and ranges of mechanical analysis results for standard sizes of coarse aggregates and screenings of aggregates used in the construction and maintenance of various types of highways. The gradation of the final composite mixture is required to conform to an approved job mix formula within the design range prescribed in Table 1 in accordance with ASTM D 448, ASTM D 1241, and ASTM D 2940, subject to the appropriate tolerances.

3. Strength requirements for stabilized road base material

After obtaining the fitting aggregates and choosing the initial cement content by weight, the specimens were prepared according to their maximum dry density and the optimum moisture

Table 1
Grading requirements for final mixtures [31].

Sieve size (square openings)	Design range (mass percentages passing)		Job mix tolerances	
	Bases	Sub-bases	Bases	Sub-bases
50 mm (2 in.)	100	100	−2	−3
37.5 mm (1 1/2 in.)	95–100	90–100	±5	+5
19.0 mm (3/4 in.)	70–92	NA	±8	NA
9.5 mm (3/8 in.)	50–70	NA	±8	NA
4.75 mm (no. 4)	35–55	30–60	±8	±10
600 μm (no. 30)	12–25	NA	±5	NA
75 μm (no. 200)	0–8	0–12	±3	±5

Table 2
Strength requirements for CTB.

Country	Other research	Compressive strength (psi)	Cement content (%)	References
	CTB	300–600		[62–64]
	CTB	750		[64,65]
	CTB	300–800		[17]
	CTB	435–870		[66,18]
	CTB	Min–500		[67]
	CTB	Min–600		[24]
South Africa		580–1160		[66,68]
United Kingdom		363–653		[69,42]
Australia		Min–435		[70,71]
China		435–725		[71,72]
New Zealand		Min–435		[73]
United States (ASTM)			3–5	[31,42,19]
United States (AASHTO)			3–5	[42,19,74]

composition. The average UCS of the cement-treated specimens cured for 7 days was measured using a hydraulic compressive strength testing machine to detect the optimum content of cement. Table 2 lists the UCS requirements of CTB subjected to curing for 7 days. It should be noted that the UCS requirements depend strongly on the road class, and the material type relies heavily on the required UCS.

4. Materials and methods

To achieve the goals of this study, three major tasks—a literature review, laboratory investigation, and data processing and analyses-were accomplished. The soil-aggregate properties were evaluated prior to the design of the mixture. The cement used was Type II Portland cement. The nontraditional stabilizer used, bitumen emulsion, is a water-based liquid emulsion and is a novel additive in this study. To evaluate the short-term performance of the stabilized soil-aggregate specimens under various stress sequences, the UCS, FS, and unsoaked CBR values were determined. The long-term performance of these specimens was investigated by subjecting them to WD cycling (durability), soaked CBR, DC, and WT tests. Finally, on the basis of the results of the data analysis, significant models were developed to demonstrate the relationship among the characteristics of the mixture.

4.1. Aggregates

Crushed granite aggregates from the Kajang Rock Quarry (Malaysia) were used as the granular base layer material in this study. Fig. 1 illustrates the grading curve of soil-aggregates within the limits specified by ASTM standards for highways and/or airports. One of the most important factors affecting the performance of CTB is its organic content. In all probability, a soil with an organic content greater than 2% or a pH lower than 5.3 will not react normally with cement [32]. A mixture pH greater than 12.0 indicates that the organics present will not interfere with hardening [33,34]. In this study, the results of a pH test conducted according to ASTM D 4972 indicated that adding cement alone to the soil-aggregate increased the pH from 8.26 to 12.13, whereas adding a cement–bitumen emulsion mixture increased the pH from 8.26 to 12.39. This clearly shows that both types of additives have a positive effect on the mixtures.

The general properties of the soil-aggregates used in this study are summarized in Table 3.

Table 3 lists the most correlated geotechnical properties of the soil-aggregates used in this study.

4.2. Portland cement

Various kinds of Portland cement have been used effectively for soil-aggregate stabilization [8,35,36]. In this study, Type II Portland cement was used as a treatment material for the granular mixtures because of its higher sulfate resistance, moderate heat of hydration, and mostly equivalent cost in comparison to other types of Portland cement. A high sulfate content of soil results in swelling and heaving problems, and it can have a deleterious influence on cementing and stabilization mechanisms. The Portland cement used in this study was required to conform to the respective standard chemical and physical requirements prescribed by ASTM C 150 and ASTM C 114. The cement would be rejected if it did not meet all of the necessary specifications. The properties of Type II Portland cement are presented in Table 4.

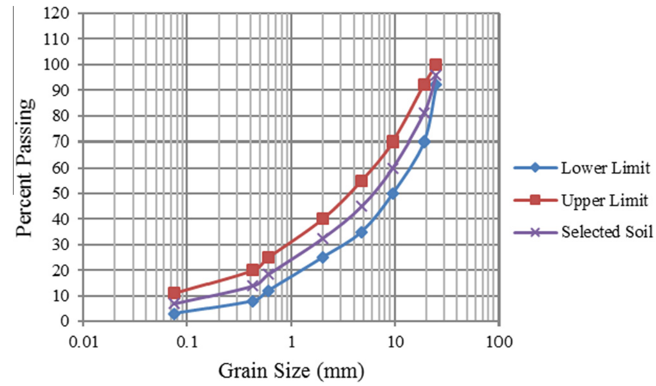

Fig. 1. Grading curves for soil-aggregate.

Table 3
Properties of soil-aggregates used in this study.

Property	Requirements	Test result	Test method
Water content (%)	NA	6.621	ASTM D 698
Unit weight (g/cm^3)	NA	2.19	ASTM D 698
pH	5.3–Min	8.26	ASTM D 4972
Unified classification	NA	GP-GM	ASTM D 2487
AASHTO classification	NA	A-1-a	ASTM D 3282/AASHTO M 145
Liquid limit (%)	25–Max	21.4	ASTM D 4318
Plastic limit (%)	29–Max	19.6	ASTM D 4318
Plastic index (%)	4–Max	1.8	ASTM D 4318
Coefficient of curvature (Cc)	NA	2.39	ASTM D 2487
Coefficient of uniformity (Cu)	NA	71.5	ASTM D 2487
Group index	NA	0	ASTM D 3282
Specific gravity (OD)	NA	2.659	ASTM C 127/C 128
Specific gravity (SSD)	NA	2.686	ASTM C 127/C 128
Apparent specific gravity	NA	2.731	ASTM C 127/C 128
Water absorption (%)	2–Max	0.973	ASTM C 127/C 128
Linear shrinkage (%)	3–Max	1.5	BS 1377: Part 2
Elongation index (%)	25–Max	13.03	BS 812: Section 105.2
Flakiness index (%)	25–Max	8	BS 812: Section 105.1
Average least dimension (mm)	NA	5.5	BS 812: Section 105.1
Sand equivalent (%)	35–Min	84	ASTM D 2419
Los Angeles abrasion (%)	50–Max	17.5	ASTM C 131
UCS (MPa)	NA	0.25	ASTM D 2166/D 1633
CBR (%)	80–Min	101.32	ASTM D 1883

4.3. Water

The mixing water used for these tests should be free of acids, alkalis, and oils, and in general it should be suitable for drinking according to ASTM D 1632 and ASTM D 4972. According to ASTD D 1193, water is classified into four grades—type I, type II, type III, and type IV—depending on its physical, chemical, and biological properties. All the mixed water used for these test methods should be ASTM type III or better. Water prepared by distillation is of type III, which is used in current study.

4.4. Bitumen emulsion

Bitumen emulsion is proposed as a polymer modifier for hydraulic cement mixtures or tile mortar adhesives. It is a surfactant-stabilized styrene–butadiene copolymer latex used in concrete, mortar, grout, and cement mixtures; when used properly (mixed well before and after use), it can produce mixtures that exhibit improved adhesion to most substrates, improved water resistance, increased

Table 4
Properties of Type II Portland cement.

Component and properties	Requirements (%)	Test result (%)	Test method
Silicon dioxide (SiO_2)	20–Min	20.18	ASTM C 150–C 114
Aluminum oxide (Al_2O_3)	6.0–Max	5.23	ASTM C 150–C 114
Calcium oxide (CaO)	Not applicable	64.40	ASTM C 150–C 114
Ferric oxide (Fe_2O_3)	6.0–Max	3.34	ASTM C 150–C 114
Magnesium oxide (MgO)	6.0–Max	1.80	ASTM C 150–C 114
Sulfur trioxide (SO_3)	6.0–Max	3.03	ASTM C 150–C 114
Loss on ignition	3.0–Max	2.17	ASTM C 150–C 114
Insoluble residue	0.75–Max	0.18	ASTM C 150–C 114
Na_2O	Not applicable	0.07	ASTM C 150–C 114
K_2O	Not applicable	0.44	ASTM C 150–C 114
Equivalent alkalies ($Na_2O + 0.658K_2O$)	0.75–Max	0.3595	ASTM C 150–C 114
Tricalcium aluminate (C_3A)	8–Max	3.21	ASTM C 150–C 114
Tricalcium silicate (C_3S)	Not applicable	53.95	ASTM C 150–C 114
Dicalcium silicate (C_2S)	Not applicable	17.32	ASTM C 150–C 114
Tetracalcium alumino-ferrite (C4AF)	Not applicable	10.16	ASTM C 150–C 114
Sum of (C_3S) and (C_3A)	58–Max	57.16	ASTM C 150–C 114
Compressive strength, MPa:			ASTM C 109/C 109 M
3 days	10–Min	27.5	
7 days	17–Min	40.3	
28 days	28–Min	57.7	
Fineness, specific surface, m^2/kg: air permeability test	280–Min	338.1	ASTM C 204
Autoclave expansion (soundness)	0.8–Max	0.5	ASTM C 151

flexural strength, increased resistance to freezing/thawing and wetting/drying cycles, and reduced water/cement ratios. The properties of bitumen emulsion are presented in Table 5.

Standard bitumen (asphalt) emulsions are brown liquids normally considered to be of the oil-in-water (O/W), made by mixing water (25–60%), bitumen (40–75%), emulsifier (0.1–2.5%) and applying mechanical energy sufficient to break the bitumen into droplets. Bitumen emulsion can be classified due to their droplets charged, pH and reactivity into cationic (positive charge, acidic), anionic (negative charge, alkaline) and nonionic types with various setting grades comprising slow setting (SS), medium setting (MS) and rapid setting (RS). Bitumen is not soluble in water so the dispersion of bitumen droplets in water is stabilized by using bitumen emulsifier. Aggregate reactivity is mostly associated with the finest particles, which contribute greatest to surface area. Thus, a reactive RS emulsion is used with low-surface-area unreactive aggregates in chip seal applications, whereas a low-reactive SS emulsion is used for a dense cold mix, which has a high content of 75 μm material, and consequently, a high reactivity. Specifications for cationic emulsified asphalt slow setting shall conform to the requirements prescribed in Table 5, according to ASTM D 244 and D 2397. The emulsified asphalt shall be homogeneous after thorough mixing, provided that separation has not occurred owing to freezing. Emulsions separated by freezing shall not be tested. Cationic slow setting (CSS) emulsions are used in combination with aggregates with high surface area to provide the desired coating and curing behavior. In addition, cationic emulsifiers have greater effects on cement hydration compared to anionic emulsifiers because of their compatibility (the addition of alkaline cement to an acidic cationic emulsion causes the pH to increase compared to the emulsion's initial pH) evaluated by emulsion stability. Furthermore, in a mixing application of dense graded aggregates, a lower viscosity of emulsion is usually required. CSS bitumen emulsion chemistry is such that it enables excellent coating and adhesion of the residual asphalt cement to aggregate surfaces in dense graded mixes because of larger average particle size, which leads to lower emulsion viscosity, as does a broad particle size distribution. In this research, with respect to the results of the coating test and cement mixing (ASTM D 244), dense graded aggregate and high adhesion between aggregates particles; a cationic slow setting (CSS-1) asphalt emulsion was chosen. It should be noted that followed by numbers indicating the emulsion viscosity ("1" meaning low viscosity). The properties of bitumen emulsion are presented in Table 5.

Table 5
Properties of bitumen emulsion.

Test on emulsions	Requirements	Test result	Test method
Viscosity, saybolt furol at 25 °C	20–100	20.9	ASTM D 2397
Storage stability test, 24–h, %	1	0.22	ASTM D 2397
Particle charge test	Positive	Positive	ASTM D 2397
Sieve test, %	0.1 Max	0.0	ASTM D 2397
Cement mixing test, %	2 Max	0.23	ASTM D 2397
Oil distillate, by volume of emulsion, %	3 Max	1.5	ASTM D 2397
Residue from distillation, %	57 Min	61.75	ASTM D 2397
Penetration, 25 °C, 100 g, 5 s, 0.1 mm	100–250	109.2	ASTM D 2397
Solubility in trichloroethylene, %	97.5 Min	99.8	ASTM D 2397
Water content	NA	58.3	ASTM D 2397

5. Experimental procedures

5.1. Moisture content–dry density relationship of the mixtures

The dry density of compacted soil-aggregate is one of the main factors influencing the strength of CTB. In addition, water is essential for achieving maximum density and for promoting the hydration of the cement. Method C of ASTM D 698 is a laboratory compaction method used to determine the relationship between the water content and the dry unit weight of soil-aggregates compacted into a 152.4-mm-diameter mold with a 24.4-N rammer dropped from a height of 305 mm, producing a compactive effort of 600 kN-m/m^3. This method was used in the present study. Specifically, three layers of soil-aggregate at a selected water content were placed in the 152.4-mm-diameter mold and each layer was compacted by 56 blows of the rammer. Further, according to ASTM D 558 Method B, the relationship between the water content and the dry density of the soil-aggregate–cement mixtures was determined using a cylindrical metal mold having a capacity of 944 cm^3 and an internal diameter of 101.60 mm. The mixtures were compacted using a 2.49 kg metal rammer having a 50.80 mm diameter dropped from a height of 305 mm. To prepare the specimens, the required amount of cement was added to the soil-aggregate in conformance to specifications ASTM C 150 and C 595, and the resulting mixture was mixed thoroughly to achieve a uniform color. Water was then added to this soil-aggregate–cement mixture and specimens were prepared by compacting this mixture in the mold in three equal layers, where each layer was compacted by 25 blows to give a total compacted depth of about 130 mm. This exact process was also applied for mixing cement with bitumen emulsion. The optimum moisture content (OMC) and maximum dry density (MDD) was determined using the compaction curve.

5.2. Unconfined compressive strength

The primary purpose of the UCS test is to determine the approximate compressive strength of a mixture that has sufficient cohesion to permit testing in the unconfined state. For this test, the mixture was prepared according to ASTM D 1632 using a metal cylinder mold with an internal diameter of 101.60 mm and a height of 116.4 mm. The specimens were placed in the molds in a moist room for 12 h for curing; subsequently, the specimens were removed using a sample extruder. The removed specimens were wrapped in plastic for protection against dripping water in the moist room at 25 °C. Three specimens were fabricated for each percent of additive, resulting in 21 samples for Portland cement (0–6%), 21 samples for bitumen emulsion (0–6%), and 18 samples for the cement–bitumen emulsion mixture. The average UCS of the specimens cured for 7, 28, and 60 days was determined using a hydraulic compressive strength testing machine by applying a load at a constant rate within the range of 140 ± 70 kPa/s according to ASTM D 1633. Finally, the unit compressive strength [MPa] was calculated by dividing the maximum load [N] by the cross-sectional area [mm^2].

5.3. Flexural strength

Flexural strength (FS) is considered a significant characteristic for pavement design and for determining slab thickness. FS is expressed as the modulus of rupture, which in this study was performed in accordance with the ASTM standard. ASTM D 1635 prescribes steps for determining the flexural strength of mixtures using a simple beam with three-point loading. In this study, the specimens were compacted into a metallic beam mold $76 \times 76 \times 290$ mm and moist-cured, as explained in Section 5.2. The average modulus of rupture of specimens cured for 7, 28, and 60 days was determined using a hydraulic testing machine. The test was conducted by applying a continuous load at a rate of 690 ± 39 kPa/min. Three specimens were fabricated for each type of additive: 4% Portland cement, 3% bitumen emulsion, and a 4% cement–3% bitumen emulsion mixture. The modulus of rupture was calculated using the following equation:

$$R = \frac{P \times L}{b \times d^2}$$

where R is the modulus of rupture [MPa], P the maximum applied load [N], L the span length [mm], b the average width of specimen [mm], and d the average depth of specimen [mm].

It should be noted that the short-term performance tests were conducted under dry-condition.

5.4. California bearing ratio

The CBR value is required for designing flexible pavement materials and thickness. In this research, the ASTM D 1883 test method was used to evaluate the potential strength of CTB and CBETB as a function of their CBR values. The specimens were compacted in five layers into a cylindrical metal mold with an inside diameter of 152.4 mm and a height of 177.8 mm to the MDD at OMC. The tests were performed for both soaked and unsoaked conditions. For soaked conditions, samples attached to a 4.54 kg steel weight were immersed in a water bath for four days to achieve suitable saturation. The initial and final measurements of swelling were taken before and after the 96-h soaking using a dial gage, and the amount of swelling was calculated as a percentage of the initial height of the samples. The average CBR of the 7-day-cured specimens was determined using a hydraulic compressive strength testing machine by applying a load at a rate of 1.27 mm/min. The load readings were recorded at a penetration of 2.5 mm to a total penetration of 7.5 mm. Then the penetration load was calculated using a testing machine-calibrated equation and the load–penetration curve was plotted. Finally, the CBR was calculated using corrected load values taken from the load–penetration curves for 2.54 mm and 5.08 mm penetration by dividing the corrected load by the standard stresses of 6.9 MPa and 10.3 MPa, respectively, and multiplying by 100. Three specimens were fabricated for each type of additive: 4% Portland cement, 3% bitumen emulsion, and a 4% cement–3% bitumen emulsion mixture.

5.5. Wetting and drying

One of the significant factors in terms of maximizing the pavement life is sufficient resistance to damage under weathering conditions such as wetting and drying. The resistance of CTB and CBETB to repeated wetting and drying cycles was performed in accordance with ASTM standards. ASTM D 559 prescribes steps for determining volume changes (swelling and shrinkage), water content changes, and soil-aggregate–cement losses, all of which were measured by subjecting hardened soil-aggregate–cement specimens to 12 WD cycles. Two identical specimens for CTB and CBETB were compacted in a cylindrical metal mold with a capacity of 944 cm^3 and internal diameter of 101.6 mm using the compaction procedure described in Section 5.1 according to ASTM D 558. The specimens were placed in the moist room and protected from free water for 7 days. They were then weighed and measured at the end of the curing period to determine their water content and volume. Then the specimens were submerged in potable water at room temperature for 5 h and then removed. The specimens were weighed and measured again to determine their volume and moisture changes. They were then placed in an oven at 71 °C for 42 h, after which they were removed, weighed, and measured. They were next subjected to two firm wire scratch brush strokes on their sides and at each end (20 brush strokes for sides and 4 strokes for each end). The specimens were then submerged in water, and this process was repeated for 12 cycles. The volume change was calculated as the percentage of the final volume of the specimen versus the original volume of the specimen at the time of molding. Both the water content of the specimen at the time of molding and the subsequent water content as a percentage of the original oven-dry weight were calculated. The soil-aggregate–cement loss was calculated as a percentage of the final oven-dry weight versus the original oven-dry weight of the specimen.

5.6. Dynamic creep

The progressive accumulation of permanent deformation of each layer of road structure under repetitious traffic load is defined as rutting. Owing to the increase in traffic loading and tire pressures, rutting has become a very important design factor because all pavement layers experience permanent deformation. Several experimental tests are used to assess the permanent deformation potential of mixtures used in pavements, i.e., dynamic creep, static creep, wheel-tracking, and marshal tests. The DC test is suitable for evaluating the permanent deformation potential of modified pavement layers because of its various outcomes [37–39]. It was employed by Monismith, Ogawa [40] in the mid-1970s. In this research, the accumulation of permanent deformation of CTB and CBETB mixtures was investigated by using the DC and WT tests. The DC test applies a repeated stress on the mixtures and measures the resulting deformation using a linear variable differential transducer (LVDT). The AS 2891.12.1 standard test sets out the method for determining resistance to permanent deformation of mixtures used in pavements subjected to vertical axis dynamic loading. This test method is used to gauge the relative performance of mixtures for pavement design by determining the rutting performance. The specimens in the current study were prepared using a cylindrical metal mold with an internal diameter of 101.6 mm. The 7-day-cured specimens with both ends capped were centrally placed between the lower and the upper load platens under a static pre-load conditioning stress of 10 kPa for 600 s using the universal testing machine (UTM-14P/5P). After removing the conditioning stress, the test was conducted by applying a haversine cyclic loading axial stress of 200 kPa at 25 °C and 50 °C for 1800 cycles, with a load cycle repeat time of 2 s (1.5 s loading and 0.5 s rest period). Three samples each of 4% cement, 3% bitumen emulsion, and 4% cement–3% bitumen emulsion mixture were prepared for DC testing. The accumulated strain for each recorded cycle was calculated using the following equation:

$$\varepsilon_{d,(n.T)} = \frac{\Delta_h}{h_0} \tag{1}$$

where $\varepsilon_{d,(n.T)}$ is the axial strain caused to the specimen after application of load n at temperature T [°C], Δ_h is the total axial deformation occurring in the specimen after the first load application [mm], and h_0 is the original height of the specimen [mm].

5.7. Wheel-tracking test

BS 598-110 specifies a method for determining the susceptibility of mixtures to plastic deformation in pavement construction under pressures similar to those experienced on the road. Three identical specimens for each mix were compacted into a cylindrical wood mold with an internal diameter of 200 mm and nominal thickness of 50 mm to the MDD at OMC. The 7-day-cured specimens were conditioned for 4 h at temperatures of 25 °C and 50 °C inside a Wessex wheel-tracking machine and then immediately prior to testing. The specimens were fixed, mounted in the clamping assembly, and fitted rigidly to the reciprocating table of the wheel-tracking machine. The machine is constructed to enable the test specimen to be moved back and forth under the loaded wheel in a horizontal fixed plane with a simple harmonic motion. The dry WT test was conducted by applying a single wheel load of 520 N through a solid rubber tire with a frequency of 21 load-cycles every 60 s, which corresponds to 42 wheel passes per minute and 230 mm of travel distance every 45 min. The total rut depth was recorded by Wessex software.

6. Results and discussion

6.1. Effect on the compatibility

Fig. 2 shows the compaction curves that demonstrate the relationship between the dry density and moisture content for the non-stabilized soil-aggregate according to ASTM D 698 and for CTB mixtures prepared with different cement contents according to ASTM D 558.

Fig. 2 shows that both the optimum water content and the maximum dry density increased with increasing cement content when the compaction moisture increased by approximately 0.25% for each 1.0% increase in the cement added to the specimen. This can be explained using the theoretical formulation of the overall void ratio of a mixture composed of soils with varying grain sizes. Lade et al. [41] showed that when small particles are added to a large-sized particle matrix, the overall void ratio decreases until all the voids are filled with small particles. This means that the dry density increases up to a specific mixing ratio of small and large particles. According to ASTM D 558, the maximum dry density of the cement–bitumen emulsion mixture was obtained at a cement content of 4% and a bitumen emulsion content of 0–6%. This parameter is used as an important variable for predicting models.

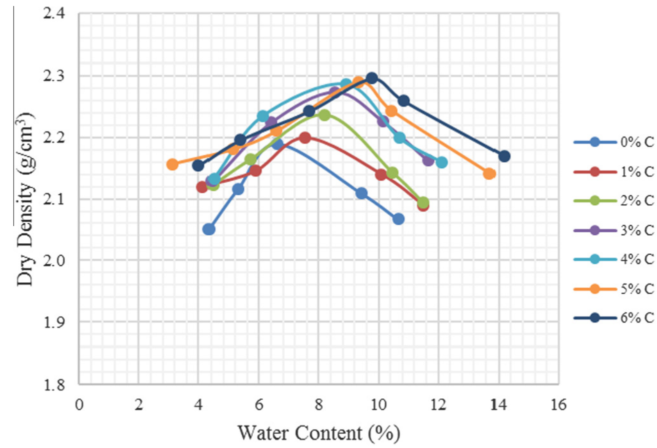

Fig. 2. Relation between moisture content and dry density for various cement contents. "C" denotes cement.

The plot of the maximum dry density versus the content of bitumen emulsion in the cement–bitumen emulsion mixture is shown in Fig. 3.

From the experimental data, the non-linear model in Fig. 3 shows the relationship between the content of bitumen emulsion in the cement–bitumen emulsion mixture and the maximum dry density as obtained for the CBETB mixture according to ASTM D 558. It is seen that the maximum dry density increases with increasing bitumen emulsion content up to 3%. However, after that, the maximum dry density decreases with increasing bitumen emulsion content on account of the higher water content of 38.23% of bitumen emulsion; this leads to a decrease in the strength of the mixture. The presence of too much water in the mixture poses a problem because it inhibits adequate compaction and decreases the toughness and flexibility of the soil-aggregate–cement structure, resulting in a decrease in the dry unit weight.

6.2. Effect on the compressive strength

The influence of the cement content, bitumen emulsion content, and curing time on the UCS of the mixture is shown in Figs. 4–6, respectively.

Fig. 4 shows the influence of the cement content on the UCS of the mixture for 7 days and 28 days of curing using two linear models based on experimental data. This figure reveals a proportional relationship between these two parameters. In other words, an

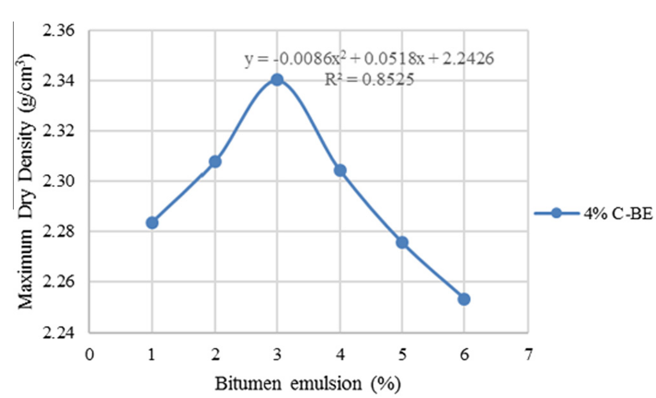

Fig. 3. Plot of maximum dry density vs. content of bitumen emulsion in the cement–bitumen emulsion mixture. "C" denotes cement and "BE" denotes bitumen emulsion; y is the maximum dry density [g/cm^3] and x is the bitumen emulsion content [%].

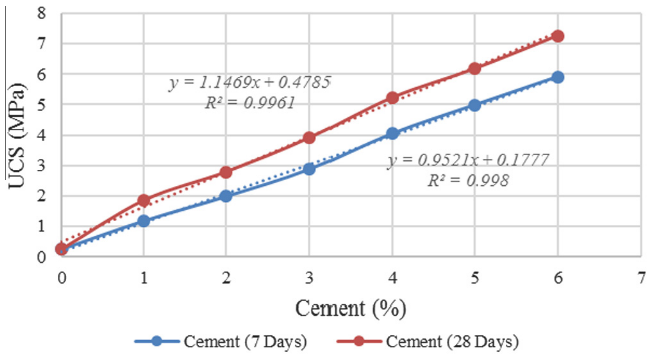

Fig. 4. Plot of UCS vs. cement content for 7 and 28 days of curing. Here, y is the UCS [MPa] and x is the time [days].

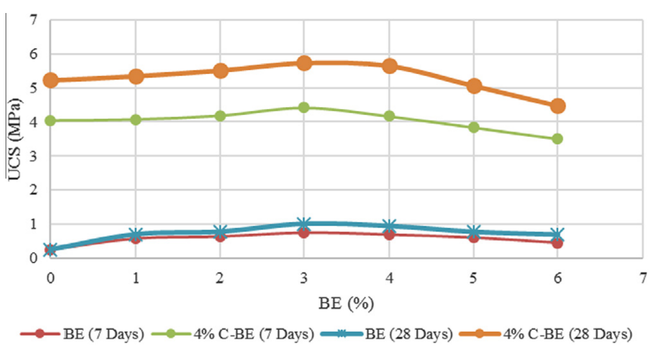

Fig. 5. Plot of UCS vs. bitumen emulsion content. Here, "BE" denotes bitumen emulsion and "C" denotes cement.

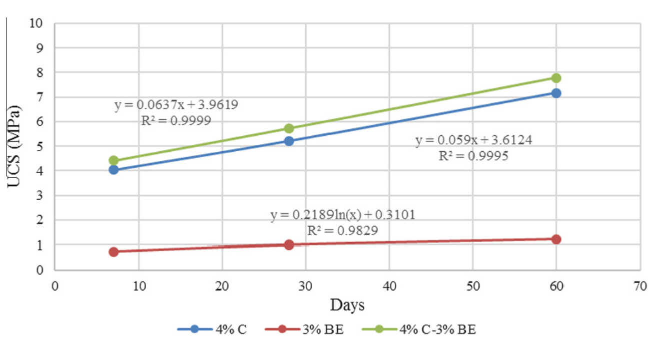

Fig. 6. Plot of UCS vs. curing time. Here, "C" denotes cement and "BE" denotes bitumen emulsion; y is the UCS [MPa] and x is the time [days].

increase in the cement content causes an increase in the UCS of the mixture on account of the hydration products of the cement, which fill the pores of the matrix and thus enhance the rigidity of its structure by forming a large number of rigid bonds in the soil-aggregate. On the basis of this graph and the strength requirements for CTB listed in Table 2, the optimum cement content was chosen as 4%.

Fig. 5 shows the influence of the bitumen emulsion content on the UCS for 7 days and 28 days of curing. It is seen that an increase in the bitumen emulsion content caused the UCS of the mixture to increase, however, at concentrations higher than 3%, the UCS decreased on account of a higher water content of 38.23% of bitumen emulsion. The mechanism of this decrease has been explained in Section 6.1. Further, the results of the UCS test reveal that it increased by 18.6% upon the addition of a 4% Portland cement–3% bitumen emulsion mixture as compared to a specimen with only 4% cement.

Fig. 6 shows the influence of curing time on the UCS via linear and nonlinear models. In this figure, it can be clearly seen that the UCS increases with increasing curing time for 4% Portland cement, 3% bitumen emulsion, and the 4% cement–3% bitumen emulsion mixture. The results indicate that the relative compressive strength obtained for 7 days of curing increased by approximately 29%, 34%, and 30%, respectively, after 28 days of curing and by 77%, 64%, and 76%, respectively, after 60 days of curing.

6.3. Influence of cement content, water content, dry density, and bitumen emulsion content on UCS

From Fig. 4, it is observed that the UCS increases linearly with increasing cement content and non-linearly with increasing dry density and bitumen emulsion content, as shown in Figs. 3 and 5, respectively. These results are in agreement with previous findings on the influence of cement content and dry density on cement-treated materials [36,42]. Xuan et al. [36] employed an adapted model to demonstrate the relationship between the UCS and the variables affecting it, i.e., the cement content, water content, and additive content.

$$f_c = K_1 \times (C/W) \times (D)^{k_2} \times e^{k_3 \times M} \quad (2)$$

where f_c is the UCS [MPa], K_1, K_2, and K_3 are adjustable variables, C is the cement content [%], D the dry density [g/cm^3], W the moisture content [%], and M the additive content [%].

Based on the experimental results, models for estimating the UCS of a mixture cured for 7 and 28 days are developed and expressed as follows:

$$f_c = 0.097 \times (C/W) \times D^{5.164} \times e^{-0.012M}, \ R^2 = 0.915 \quad (3)$$

$$f_c = 0.120 \times (C/W) \times D^{5.245} \times e^{-0.013M}, \ R^2 = 0.855 \quad (4)$$

where M is the bitumen emulsion content [%].

6.4. Influence of curing time

Curing time is another important factor affecting UCS. Fig. 6 shows UCS as a function of curing time at a cement content of 4%. It can be seen that UCS increased almost linearly with increasing curing time. A number of studies have reported the influence of curing time on UCS [6,43–46]. For example, the relationship between UCS and curing time can be given as in [47].

$$f_c(t) = f_c(t_0) + k_1 \times \log(t/t_0) \quad (5)$$

where $f_c(t)$ is UCS at a curing age of t [days] and $f_c(t_0)$ is UCS at a curing age of t_0 [days]. There is another adapted prediction model that considers the influence of curing time on UCS, which was proposed by Lim and Zollinger [48], as given in Eq. (5). This model is based on the calibration of the American Concrete Institute (ACI) Committee model, which introduces two adjustable variables (k_1 and k_2) for UCS estimation.

$$f_c(t) = f_c(28) \times \frac{t}{k_1 + k_2 \times t} \quad (6)$$

where $f_c(28)$ is the 28-day UCS. Herein, the relationship between the UCS and the curing time is expressed as in Eq. (7) using three adjustable variables (k_1, k_2, and k_3):

$$f_c(t) = k_1 \times k_2^{f_c(28)} \times t^{(k_3)} \quad (7)$$

Thus far, there are three models reported for RBS that consider the influence of curing time, such as the exponential model, the log-scale model, and the ACI model, expressed in Eqs. (8)–(10), respectively [36,48,49]:

$$f_c = k_1 \times (C/W) \times D^{k_2} \times e^{(k_3.M)} \times e^{\left[1-(28/t)^{k_4}\right]} \tag{8}$$

$$f_c = k_1 \times (C/W) \times D^{k_2} \times e^{(k_3.M)} \times [1 + k_4 \times \log(t/28)] \tag{9}$$

$$f_c = k_1 \times (C/W) \times D^{k_2} \times e^{(k_3.M)} \times t/(5.1 + k_4 \times t) \tag{10}$$

Based on the experimental data derived from the present work, the above three estimation models are expressed as in Eqs. (11)–(13), respectively:

$$f_c(t) = 0.123 \times (C/W) \times D^{5.216} \times e^{(-0.013M)} \times e^{\left[1-(28/t)^{0.174}\right]},\ R^2 = 0.966 \tag{11}$$

$$f_c(t) = 0.123 \times (C/W) \times D^{5.216} \times e^{-0.013M} \times [1 + 0.396 \times \log(t/28)],\quad R^2 = 0.966 \tag{12}$$

$$f_c(t) = 0.214 \times (C/W) \times D^{5.216} \times e^{-0.013M} \times t/(5.1 + 1.564 \times t),\quad R^2 = 0.966 \tag{13}$$

6.5. Effect on the modulus of rupture

Three samples each of 4% cement, 3% bitumen emulsion, and 4% cement–3% bitumen emulsion mixture were prepared for testing to determine the flexural strength after 7, 28, and 60 days of moist-curing using a simple beam with a three-point loading method. The FS results are presented in Fig. 7.

Fig. 7 shows the values of FS versus days for curing times of 7, 28, and 60 days. The results show that the value of FS increased with increasing curing time, which indicates that curing time is an important factor in CBETB. The use of the 4% cement–3% bitumen emulsion mixture increased the FS by 81.4% and 288.2% as compared to the use of 4% cement and 3% bitumen emulsion, respectively. The figure also shows the influence of curing time on FS using linear and non-linear models, where y is FS [MPa] and x is the time [days]. FS and UCS are critical material parameters as input data for CTB in pavement design methods such as American association of state highway and transportation (AASHTO) and mechanistic–empirical pavement design guide (MEPDG) methods [50,51]. In most circumstances, the modulus of rupture is specified by the existing relationship between UCS and FS. For example, in the ACI model, $M_{rup} = 7.5\sqrt{f_c}$, whereas in the U.S. Army Corps of Engineers (USACE) model, $M_{rup} = 9.046\sqrt{f_c}$ [24] and $M_{rup} = af_c - b$ [52], where M_{rup} is the modulus of rapture. For the modulus of rupture, it has been shown from previous studies that the FS of CTB is usually about 15–30% of the UCS [17,52,53]. Fig. 8 compares FS to UCS. The linear models

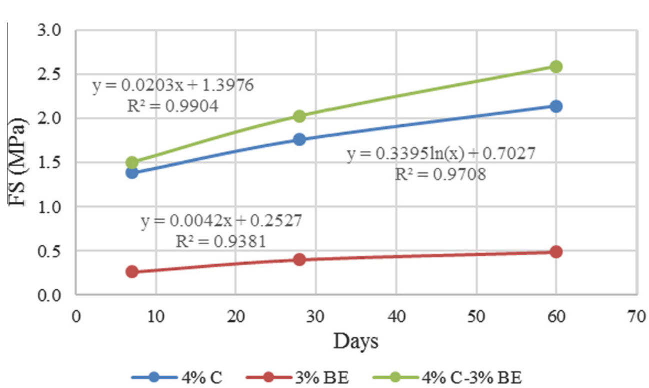

Fig. 7. Plot of FS vs. curing time. Here, "C" denotes cement and "BE" denotes bitumen emulsion; y is the FS [MPa] and x is the time [days].

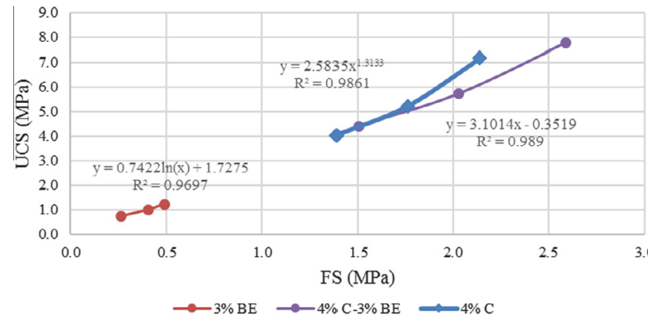

Fig. 8. The relationship between UCS and FS. Here, "C" denotes cement and "BE" denotes bitumen emulsion; y is the UCS [MPa] and x is the FS [MPa].

indicate that the average FS of CTB and CBETB for 7–60 days of curing is 32.6% and 34.2% of UCS, respectively.

6.6. Effect on the California bearing ratio

In this study, the improvement of the soil-aggregate was investigated with the inclusion of Portland cement only, bitumen emulsion only, and a Portland cement–bitumen emulsion mixture. To express the saturated and unsaturated conditions for different field applications, the CBR was evaluated for soaked and unsoaked samples. The influence of the cement content, bitumen emulsion content, and cement–bitumen emulsion mixture on the CBR are shown in Fig. 9.

The results from samples treated with 4% cement, 3% bitumen emulsion, and the 4% cement–3% bitumen emulsion mixture are summarized in Fig. 9 in terms of CBR performance versus depth of penetration for both unsoaked and 4-day soaked conditions. From the figure, it is clear that the best improvement for both soaked and unsoaked conditions was obtained from the 4% cement–3% bitumen emulsion mixture. The average CBR of 4% cement, 3% bitumen emulsion, and the 4% cement–3% bitumen emulsion mixtures are 289.7%, 129.2%, and 308.4%, respectively, for unsoaked conditions and 292.6%, 84.68%, and 315.67%, respectively, for the 4-day soaked condition. This result indicates that use

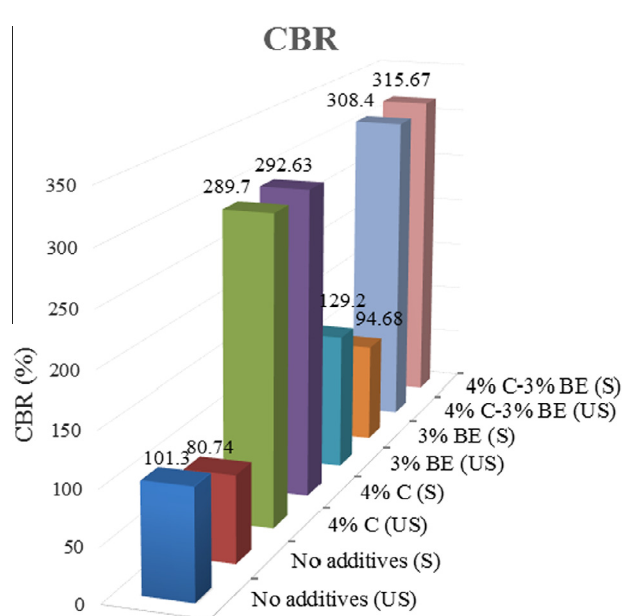

Fig. 9. CBR test results for the mixtures. Here, "C" denotes cement and "BE" denotes bitumen emulsion; US denotes unsoaked and S denotes soaked.

of the 4% cement–3% bitumen emulsion mixture increases the CBR by 7% and 139% as compared to the use of 4% cement and 3% bitumen emulsion, respectively. Further, it can be seen from Fig. 9 that the effect of the 4-day soaked condition on the CBR value was negligible for all modified specimens except the samples with no additives and 3% bitumen emulsion, in which the soaked CBR value decreased by 25.4% and 36.4%, respectively, as compared to the unsoaked condition. In this study, the results of the swelling tests are less than 0.10%, which can be considered negligible. The average swelling potential of the soil-aggregate compaction with no additives at OMC was 0.031%, whereas the average swelling potential of 4% cement, 3% bitumen emulsion, and the 4% cement–3% bitumen emulsion mixture was 0.017%, 0.023%, and 0.013%, respectively. This result indicates that the addition of the additives to soil-aggregate samples lowered the swelling potential; however, use of the 4% cement–3% bitumen emulsion mixtures reduced the swelling potential by 30.7% as compared to the use of 4% cement. The soil-aggregate used in this study was a low-plasticity silt, and it did not present a notable swelling problem even without treatment.

6.7. Durability of stabilized soil-aggregate

The results of the WD tests are shown in Figs. 10–12 for cement, bitumen emulsion, and cement–bitumen emulsion mixture, respectively.

Figs. 10–12 show the results of soil-aggregate–cement losses, water content changes, and volume changes for 4% cement, 3% bitumen emulsion, and the 4% cement–3% bitumen emulsion mixture, respectively, induced by subjecting hardened soil-aggregate–cement specimens to 12 WD cycles. From the figures, it is clear that the average water absorptions of 4% cement, 3% bitumen emulsion, and the 4% cement–3% bitumen emulsion mixture was 4.842%, 5.127%, and 2.67%, respectively, for each WD cycle. This result indicates that use of the 4% cement–3% bitumen emulsion mixture reduced the water absorption in each cycle by 179.4% as compared to the use of only cement in the mixture. Further, the average volume change of 4% cement, 3% bitumen emulsion, and the 4% cement–3% bitumen emulsion mixture was 0.572%, 3.15%, and 0.223%, respectively, for each WD cycle. This result indicates that use of the 4% cement–3% bitumen emulsion mixture reduced the volume change in each cycle by 256.3% as compared to the use of only cement in the mixture. Finally, it is seen from the figures that the average weight changes of 4% cement, 3% bitumen emulsion, and the 4% cement–3% bitumen emulsion mixture were 0.407%, 2.16%, and 0.192%, respectively, for each WD cycle. This result indicates that use of the 4% cement–3% bitumen emulsion mixture reduced the weight change in each cycle by 211.95% as compared to the use of only cement in the mixture. It should be noted that the soil-aggregate sample without any additive failed in cycle 1 because of 100% water absorption, 100% volume change, and 100% weight loss.

Figs. 13 and 14 show the results of the total volume change and total soil-aggregate–cement losses for 4% cement, 3% bitumen emulsion, and the 4% cement–3% bitumen emulsion mixture induced by subjecting hardened soil-aggregate–cement specimens to 12 WD cycles. It is seen that the total volume changes of cement, bitumen emulsion, and the cement–bitumen emulsion mixture were 6.87%, 32.25%, and 2.68%, respectively, after 12 WD cycles. Further, the total weight changes of cement, bitumen emulsion, and the cement–bitumen emulsion mixture were found to be 4.885%, 27.52%, and 2.31%, respectively, after 12 WD cycles. The results show that the addition of the 4% Portland cement–3% bitumen emulsion mixture resulted in a 179.4% reduction in water

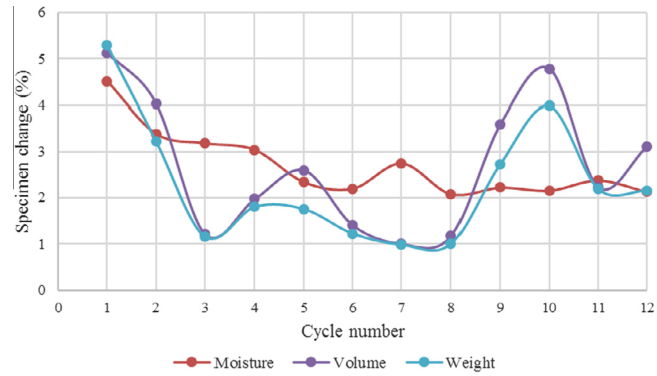

Fig. 11. Moisture, volume, and weight changes of bitumen emulsion over 12 WD cycles.

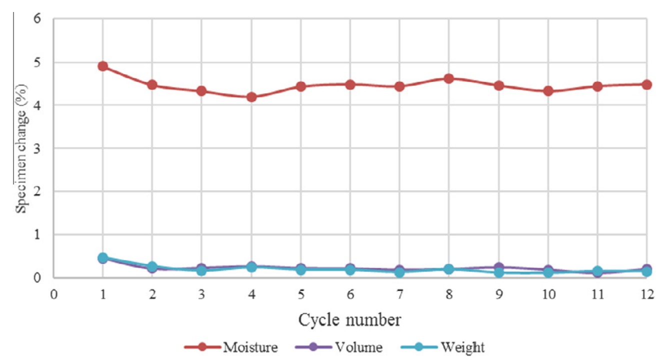

Fig. 12. Moisture, volume, and weight changes of cement–bitumen emulsion mixture over 12 WD cycles.

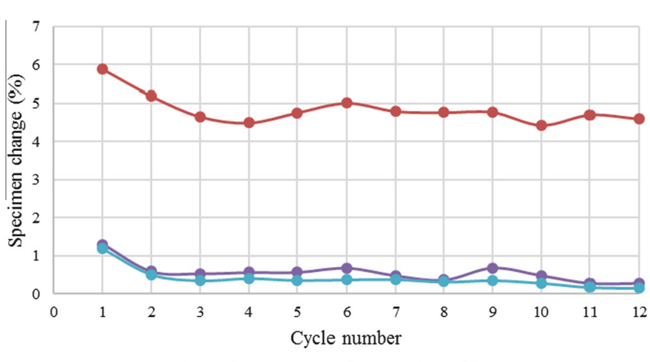

Fig. 10. Moisture, volume, and weight changes of cement over 12 WD cycles.

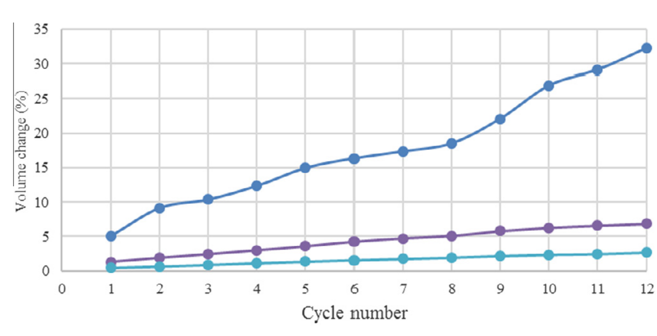

Fig. 13. Total volume change over 12 WD cycles. Here, "C" denotes cement and "BE" denotes bitumen emulsion.

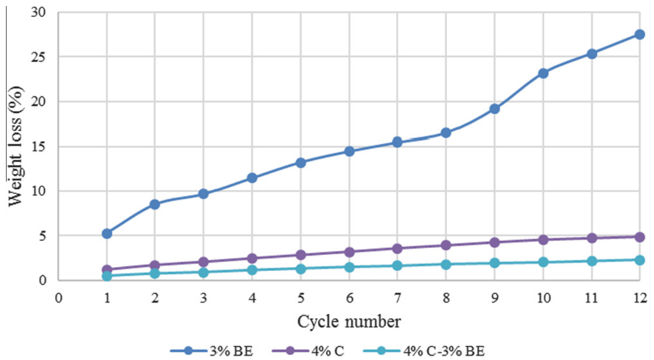

Fig. 14. Total weight loss over 12 WD cycles. Here, "C" denotes cement and "BE" denotes bitumen emulsion.

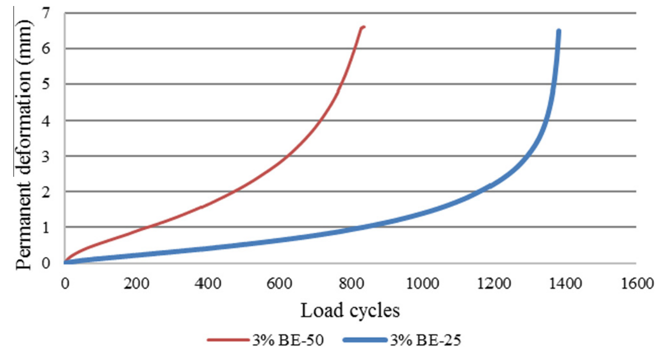

Fig. 16. Cumulative permanent strain vs. load cycles. Here, "BE" denotes bitumen emulsion, 25 and 50 denote 25 °C and 50 °C.

absorption, a volume change of 256.3%, and a weight change of 211.95% as compared to the specimen with only 4% cement after 12 WD cycles. In later studies, Shojaei Baghini et al. [35] investigated the same test method on a mixture using a polymer emulsion (4% Portland cement–8% carboxylated styrene–butadiene emulsion), which resulted in a better improvement in water absorption, volume change and weight change as compared to the specimen with 4% Portland cement–3% bitumen after 12 WD cycles. It should be noted that the linear shrinkage test was done on the mixture. The result of this test showed linear shrinkage decreases of 60% due to the addition of 4% Portland cement–3% bitumen emulsion as compared to a sample with only 4% cement. However, it requires more research on shrinkage cracks. Permanent deformation of stabilized soil-aggregate

6.7.1. Dynamic creep

The mixtures were prepared using various additives and their permanent deformation was compared with each other. In order to have a better understanding of the rutting behavior of the CBETB at different environmental temperatures, DC tests were carried out at temperatures of 25 and 50 °C. Figs. 15 and 16 illustrate the results for samples tested under at stress level of 200 kPa. The figure shows that adding 4% cement–3% bitumen emulsion to the mixture remarkably decreased its susceptibility to permanent deformation, resulting in significant enhancement of the performance of the modified mixture. However, the results show that when the environmental temperature increased from 25 °C to 50 °C, the strain had almost no effect on the permanent deformation potential for all modified specimens except the samples with 3% bitumen emulsion, in which the permanent deformation value has significant effect on the mixture as shown in Fig. 16. The 3% bitumen emulsion specimen is failed after nearly 800 load cycle when the strain value reach 6.619 mm at 25 °C and the specimen is failed after nearly 1300 load cycle when the strain value reach 6.497 mm at 50 °C. This result indicates that use of the 4% cement–3% bitumen emulsion mixture reduced the permanent deformation by 23.5% and 1682% as compared to the use of cement and bitumen emulsion, respectively.

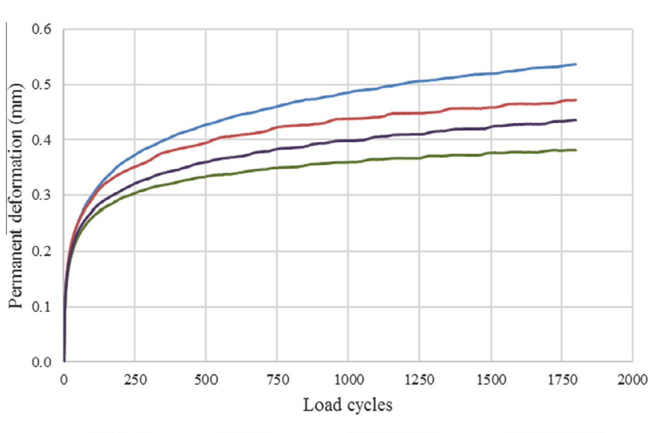

Fig. 15. Cumulative permanent strain vs. load cycles. Here, "C" denotes cement and "BE" denotes bitumen emulsion, 25 and 50 denote 25 °C and 50 °C.

6.7.2. Wheel-tracking tests

The rutting behavior of the compacted mixture was simulated using a Wessex wheel-tracking tester. Twelve samples (4% cement, 3% bitumen emulsion, and 4% cement–3% bitumen emulsion mixture) were prepared, cured at 25 °C for 7 days and tested dry under the wheel load at 25 °C and 50 °C. To achieve the specified temperature, the samples were kept in the wheel-tracking machine for 4 h. The results of WT test are given in Figs. 17 and 18, which show rut depth versus load cycles. The results indicate that the sample with 3% bitumen emulsion had the most rutting; however, the use of the 4% cement–3% bitumen emulsion mixture resulted in a reduction in rut depth of 36.7% and 705%, respectively, at 50 °C, and 38% and 483%, respectively, at 25 °C as compared to samples with cement and bitumen emulsion, respectively.

6.7.3. Three-stage permanent deformation behavior

Several rutting prediction models have been proposed since the 1970s: the semi-log model, $\log \varepsilon_p = C_0 + C_1(\log N) + C_2(\log N)^2 + C_3(\log N)^3$, the power law model, $\varepsilon_p = aN^b$ [40], the VESYS model, $\varepsilon_p = \mu\varepsilon_r N^{-\alpha}$ [37], the Ohio State model, $\varepsilon_p = aN^{1-m}$ [54], Tseng and Lytton's model, $\varepsilon_p = \varepsilon_0 e^{-(\rho/N)^\beta}$ [55], the Superpave model, $\log \varepsilon_p = \log \varepsilon_p(1) + S \log N$ [56], and the

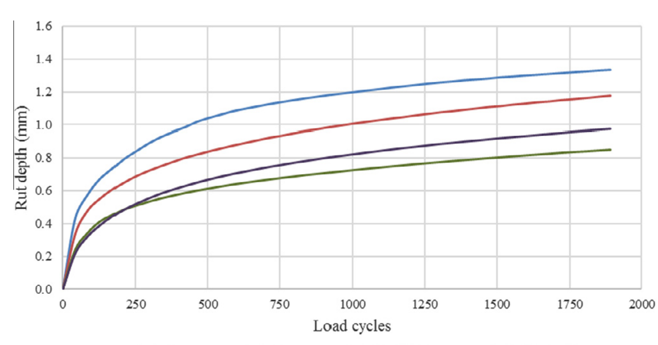

Fig. 17. Rut depth vs. load cycles. Here, "C" denotes cement and "BE" denotes bitumen emulsion, 25 and 50 denote 25 °C and 50 °C.

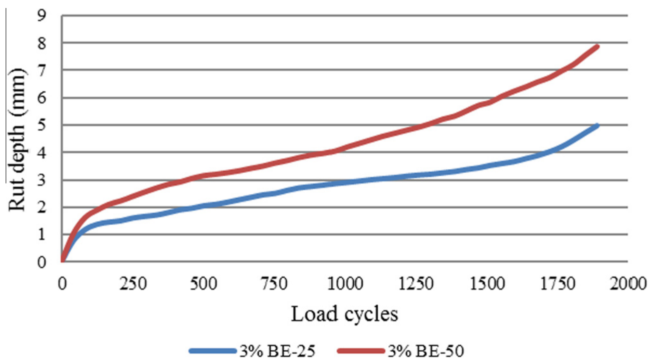

Fig. 18. Rut depth vs. load cycles. Here, "BE" denotes bitumen emulsion, 25 and 50 denote 25 °C and 50 °C.

AASHTO 2002 model, $\log \frac{\varepsilon_p}{\varepsilon_r} = \log C + 0.4262 \log N$, $C = \frac{T^{2.02755}}{5615.391}$ [57], where ε_p is the accumulated permanent strain, N the number of load repetitions, ε_r the resilient strain, $\varepsilon_p(1)$ the permanent strain at the first load application, μ the permanent deformation parameter representing the constant of proportionality between the permanent strain and elastic strain, α the permanent deformation parameter indicating the rate of decrease in incremental permanent deformation as the number of load repetitions increases, C a function of temperature (°F), and a, b, s, β, ε_0, C_0, C_1, C_2, C_3, and m are regression constants. It should be noted that for creep test results in general, the cumulative permanent strain is composed of three stages, namely, the primary, secondary, and tertiary stages, as shown in Fig. 19. The strain rate decreases during the primary stage until reaching a constant value, which is defined as the onset of the secondary stage. During the secondary stage, the rate of strain remains almost constant, and finally it increases during the tertiary phase, which is due to significant deformation of the samples by the load application.

The abovementioned models appear to adequately characterize only the primary stage and none of them can describe effectively the secondary and/or tertiary stages. Based on the definition of the three-stage permanent deformation curve, a complete three-stage model was proposed by Zhou in 2004, with one model for each phase, namely, a power-law model for the primary stage, a linear model for the secondary stage, and an exponential model for the tertiary stage, as shown in the following equations [59]:

$$\text{Primary stage}: \quad \varepsilon_p = aN^b, \ N \leqslant N_{PS} \tag{14}$$

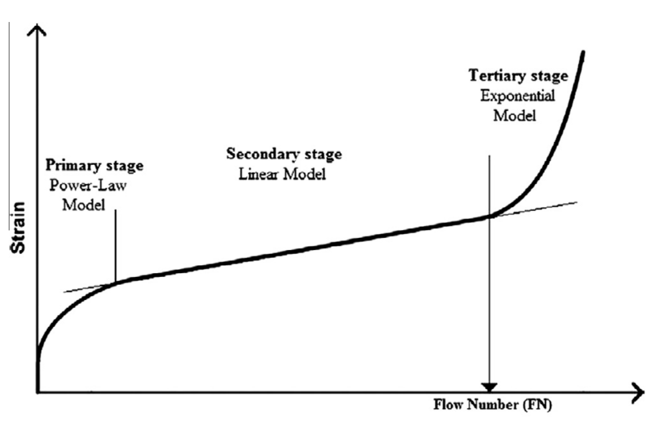

Fig. 19. Typical creep curves [58].

$$\text{Secondary stage}: \quad \varepsilon_p = \varepsilon_{PS} + c(N - N_{PS}), \ N_{PS} \leqslant N \leqslant N_{ST}, \ \varepsilon_{PS} = aN_{PS}^b \tag{15}$$

$$\text{Tertiary stage}: \quad \varepsilon_p = \varepsilon_{ST} + d\left(e^{f(N-N_{ST})-1}\right), \ \varepsilon_{ST} = \varepsilon_{PS} + c(N_{ST} - N_{PS}), \ N_{ST} \leq N \tag{16}$$

where N_{PS} is the number of load repetitions corresponding to the initiation of the secondary phase, N_{ST} the number of load repetitions corresponding to the initiation of tertiary phase, ε_{PS} the permanent strain corresponding to the initiation of the secondary phase, ε_{ST} the permanent strain corresponding to the initiation of the tertiary phase, and a, b, c, d and f are material constants. This model seems to have a better correlation with permanent deformation in the field as compared to other models because each transition point of the creep curve can be obtained by using this model. West et al. developed a three-stage model, but they could not estimate the boundary points of the creep curve stages [60]. In later studies, Khodaii and Mehrara [61] and Baghaee Moghaddam et al. [58] used Zhou's model to investigate the strain of styrene–butadiene–styrene- and polyethylene terephthalate-modified asphalt mixtures, respectively, evaluating the boundary point for each stage. In the current study, to have a better understanding of the permanent deformation of the mixtures, the Zhou three-stage model was used. MATLAB software was used for modeling each phase in order to find the transition point between each stage. Tables 6 and 7 present the results of the three-stage model for the mixtures based on the creep and wheel-tracking curves. As can be seen in Table 6, the creep curve mixtures enter the first and second stages; however, they do not go through the third stage. This may be because of the lower number of cyclic loads as compared to Khodaii and Mehrara [61] and Baghaee Moghaddam et al. [58]; their mixtures passed the tertiary stage in the creep curve. Table 7 shows the rut depth based on the wheel-tracking curve, which is similar to the creep curve.

7. Conclusion and recommendation

In this study, the long-term performance of CTB and CBETB was investigated via WD, DC, WT, and soaked CBR tests and the short-term performance was investigated via UCS, CBR, and FS tests. The results of the tests show that the strength increased with increasing bitumen emulsion content up to 3%, after which it decreased. This might be due to the water content of bitumen emulsion (38.23%), which caused a reduction in the dry density and strength of the mixture. The test results showed that application of CBETB to a soil-aggregate is an effective treatment for improving its strength and permanent deformation, reducing its water vulnerability, and increasing the bearing capacity of the pavement, all of which result in a significant increase in the lifetime of the pavement. In addition, the total number of roadway layers can be reduced by using CBETB because of its higher bearing capacity, which effectively reduces the construction time and cost. The results of the long-term tests showed that the Portland cement–bitumen emulsion mixture considerably improves the permanent deformation potential and the resistance of CBETB to moisture damage, and it reduces both soil-aggregate–cement losses and volume changes. This implies that introducing Portland cement and bitumen emulsion into soil-aggregate mixtures reduce their moisture susceptibility because both of these components are effective adhesive agents for mixtures. Tables 8 and 9 show the summary results of UCS, FS, unsoaked CBR, soaked CBR, WD, DC and WT.

From this study, and based on the analysis of the results of Tables 8 and 9, the following considerations and recommendations can be drawn:

Table 6
Three-stage model for the mixtures based on the creep curve.

Temperature (°C)	Additives	Primary stage		Secondary stage		Tertiary stage
		Model	End point	Model	End point	Model
25	4% C	$\varepsilon_p = 104.203N^{0.22}$	420	$\varepsilon_p = 393.546 + 0.081(N - 420)$	[a]	[a]
	4% C–3% BE	$\varepsilon_p = 108.785N^{0.183}$	570	$\varepsilon_p = 347.435 + 0.029(N - 570)$	[a]	[a]
50	4% C	$\varepsilon_p = 106.791N^{0.223}$	830	$\varepsilon_p = 478.0.67 + 0.062(N - 830)$	[a]	[a]
	4% C–3% BE	$\varepsilon_p = 98.13951N^{0.215}$	360	$\varepsilon_p = 347.894 + 0.086(N - 360)$	[a]	[a]

[a] Not found at the end of 1800 load cycle.

Table 7
Three-stage model for the mixtures based on the wheel-tracking curve.

Temperature (°C)	Additives	Primary stage		Secondary stage		Tertiary stage
		Model	End point	Model	End point	Model
25	4% C	$\varepsilon_p = 132.669N^{0.295}$	1134	$\varepsilon_p = 1056.53 + 0.156(N - 1134)$	[b]	[b]
	4% C–3% BE	$\varepsilon_p = 87.508N^{0.314}$	672	$\varepsilon_p = 675.837 + 0.153(N - 672)$	[b]	[b]
50	4% C	$\varepsilon_p = 172.143N^{0.285}$	1050	$\varepsilon_p = 1250.05 + 0.091(N - 1050)$	[b]	[b]
	4% C–3% BE	$\varepsilon_p = 68.715N^{0.363}$	1008	$\varepsilon_p = 845.878 + 0.150(N - 1008)$	[b]	[b]

[b] Not found at the end of 1800 load cycle.

Table 8
Summary of UCS, FS and U-CBR test results.

Curing (days)	Sample ID	UCS (MPa)	FS (MPa)	U-CBR (%)
7	3% B	0.75	0.26	129.2
	4% C	4.05	1.39	289.7
	4% C–3% B	4.42	1.5	308.4
28	3% B	1.02	0.40	NA
	4% C	5.22	1.76	NA
	4% C–3% B	5.73	2.03	NA
60	3% B	1.23	0.49	NA
	4% C	7.17	2.14	NA
	4% C–3% B	7.79	2.56	NA

Table 9
Summary of S-CBR, WD, DC, and WT test results.

Sample ID	WD (%)		DC (mm)		WT (mm)		S-CBR (%)
	Weight	Volume	25 °C	50 °C	25 °C	50 °C	
3% B	27.52	32.25	6.65	6.62	4.98	7.87	84.68
4% C	4.885	6.863	0.473	0.536	1.177	1.336	292.63
4% C–3% B	2.31	2.68	0.382	0.435	0.853	0.977	315.67

1. CBETB has been shown to have excellent potential for use as a modifier in road base construction with a high load-spreading capacity.
2. Based on the study findings, the use of 4% cement and 3% bitumen emulsion in the pavement base layer are recommended.
3. The results showed that the addition of Portland cement and bitumen emulsion significantly increased the compressive strength, flexural strength, pH, and CBR of the mixture.
4. The UCS, FS, and CBR values increased by 18.6%, 81.4%, and 7%, respectively, upon the addition of a 4% Portland cement–3% bitumen emulsion mixture as compared to the specimen with only 4% cement.
5. The WD cycling (durability) tests showed that the addition of the 4% Portland cement–3% bitumen emulsion mixture resulted in reductions of 179.4% water absorption, a volume change of 256.3%, and a weight change of 211.95% as compared to the specimen with only 4% cement after 12 WD cycles.
6. Both DC and WT tests indicated that the permanent deformation characteristics of CBETB remarkably improved as compared to the control mixture at the different environmental temperature conditions.
7. Three estimation models for the UCS of CBETB were developed in terms of mixture variables such as the cement content, water content, dry density, bitumen emulsion content, and curing time, and the Zhou three-stage model was developed for DC and WT in order to show the permanent deformation behavior of the mixtures on CBETB.
8. It is recommended that other CBETB structural properties should also be considered, including microstructure analysis using scanning electron microscopy (SEM) and energy dispersive X-ray (EDX) tests. This subject is under investigation by the authors and will be the subject of another paper to be published.

Acknowledgements

The authors would like to thank the Sustainable Urban Transport Research Centre (SUTRA) at the Faculty of Engineering and Built Environment of Universiti Kebangsaan Malaysia (UKM) for providing research facilities. The authors also would like to acknowledge UKM for providing research funding through project DLP-2014-010. Finally, the authors are grateful to the University of Malaya (UM) for experimental collaboration.

References

[1] R. Goodary, G.L. Lecomte-Nana, C. Petit, D.S. Smith, Investigation of the strength development in cement-stabilised soils of volcanic origin, Constr. Build. Mater. 28 (1) (2012) 592–598.
[2] O.S.B. Al-Amoudi, K. Khan, N.S. Al-Kahtani, Stabilization of a Saudi calcareous marl soil, Constr. Build. Mater. 24 (10) (2010) 1848–1854.
[3] E.A. Basha, R. Hashim, H.B. Mahmud, A.S. Muntohar, Stabilization of residual soil with rice husk ash and cement, Constr. Build. Mater. 19 (6) (2005) 448–453.
[4] S. Horpibulsuk, R. Rachan, A. Chinkulkijniwat, Y. Raksachon, A. Suddeepong, Analysis of strength development in cement-stabilized silty clay from microstructural considerations, Constr. Build. Mater. 24 (10) (2010) 2011–2021.
[5] F. Sariosseiri, B. Muhunthan, Effect of cement treatment on geotechnical properties of some Washington State soils, Eng. Geol. 104 (1) (2009) 119–125.
[6] A. Ismail, M.S. Baghini, M.R. Karim, F. Shokri, R.A. Al-Mansob, A.A. Firoozi, et al., Laboratory investigation on the strength characteristics of cement-treated base, Appl. Mech. Mater. 507 (3) (2014) 353–360.
[7] D.R. Salomon, Asphalt emulsion technology, in: Transportation Research Board, Characteristics of Bituminous Materials Committee, Transportation Research Circular E-C102, Washington, DC, 2006.
[8] S. Brown, D. Needham, A study of cement modified bitumen emulsion mixtures, Asphalt Paving Technol. 69 (2000) 92–121.

[9] F. Wang, Y. Liu, S. Hu, Effect of early cement hydration on the chemical stability of asphalt emulsion, Constr. Build. Mater. 42 (2013) 146–151.
[10] D. Lesueur, J.J. Potti, Cold mix design: a rational approach based on the current understanding of the breaking of bituminous emulsions, Road Mater. Pavement Des. 5 (sup1) (2004) 65–87.
[11] C.-T. Lu, M.-F. Kuo, D.-H. Shen, Composition and reaction mechanism of cement–asphalt mastic, Constr. Build. Mater. 23 (7) (2009) 2580–2585.
[12] A. Grilli, A. Graziani, M. Bocci, Compactability and thermal sensitivity of cement–bitumen-treated materials, Road Mater. Pavement Des. 13 (4) (2012) 599–617.
[13] W.G. Wong, Y. Qun, K.C.P. Wang, Performances of asphalt-treated base and semi-rigid base, HKIE Trans. 10 (3) (2003) 54–58.
[14] I. Pérez, L. Medina, M.Á. del Val, Mechanical properties and behaviour of in situ materials which are stabilised with bitumen emulsion, Road Mater. Pavement Des. 14 (2) (2013) 221–238.
[15] E. Horak, E.M. Mukandila, Exploratory use of Rigden voids as design criteria for the design of sand treated with emulsion, Road Mater. Pavement Des. 9 (3) (2008) 525–535.
[16] S.M. Marandi, P. Safapour, Base course modification through stabilization using cement and bitumen, Am. J. Appl. Sci. 6 (1) (2009) 30–42.
[17] S. Garber, R.O. Rasmussen, D. Harrington, Guide to Cement-based Integrated Pavement Solutions, Institute for Transportation, Portland Cement Association, Iowa State University, US, 2011.
[18] C.R. Freeme, J.H. Maree, A.W. Viljoen, Mechanistic Design of Asphalt Pavements and Verification Using the Heavy Vehicle Simulator, National Institute for Transport and Road Research, Pretoria, South Africa, 1982.
[19] D. Xuan, Literature Review of Research Project: Structural Properties of Cement Treated Materials, Section Road and Railway Engineering, Delft University of Technology, Netherland, 2009.
[20] F. Bell, Engineering Treatment of Soils, E & FN Spon: Taylor & Francis, London, 2002.
[21] Ş. Eren, M. Filiz, Comparing the conventional soil stabilization methods to the consolid system used as an alternative admixture matter in Isparta Darıdere material, Constr. Build. Mater. 23 (7) (2009) 2473–2480.
[22] P. Pérez, F. Agrela, R. Herrador, J. Ordoñez, Application of cement-treated recycled materials in the construction of a section of road in Malaga, Spain, Constr. Build. Mater. 44 (2013) 593–599.
[23] NITRR, Cementitious Stabilizers in Road Construction: National Institute for Transport and Road Research, South Africa, Highway Materials Committee, Committee of State Road Authorities, 1986.
[24] PCA, Soil-Cement Laboratory Handbook (ASTM/AASHTO Soil-Cement Testing procedures), Portland Cement Association, Cornell University, Skokie, IL 60077 USA, 1992.
[25] M. Shojaei Baghini, A. Ismail, B. Kheradmand, M.H. Hafezi, R. Alezzi Almansob, Bitumen-cement stabilized layer in pavement construction using indirect tensile strength (ITS) method, Res. J. Appl. Sci., Eng. Technol. 5 (24) (2013) 5652–5656.
[26] R. Terrell, C. Wang, Early curing behavior of cement modified asphalt emulsion mixtures, Assoc. Asphalt Paving Technol. 40 (1971) 108–125.
[27] R. Schmidt, L. Santucci, L. Coyne, Performance characteristics of cement-modified asphalt emulsion mixes, Assoc. Asphalt Paving Technol. 42 (1973) 300–319.
[28] R.W. Head, An informal report of cold mix research using emulsified asphalt as a binder, Assoc. Asphalt Paving Technol. 43 (110–131) (1974).
[29] Y. Niazi, M. Jalili, Effect of Portland cement and lime additives on properties of cold in-place recycled mixtures with asphalt emulsion, Constr. Build. Mater. 23 (3) (2009) 1338–1343.
[30] M. Bocci, A. Grilli, F. Cardone, A. Graziani, A study on the mechanical behaviour of cement–bitumen treated materials, Constr. Build. Mater. 25 (2) (2011) 773–778.
[31] ASTM, American Society for Testing and Materials (ASTM), West Conshohocken, Pa, USA, 2004.
[32] ACI, State-of-the-art report on soil cement, ACI Mater. J. 87 (4) (1997) 395–417.
[33] ARMY, Soil stabilization for pavements, TM 5-822-14, Department of the Army, the Navy and the Air Force, Washington, DC, 1994.
[34] D. Jones, D. Jones, Guidelines for the Stabilization of Subgrade Soils in California, California: UCD-ITS-RR-10-38, Institute of Transportation Studies, University of California, Davis, 2010.
[35] M. Shojaei Baghini, A. Ismail, M.R. Karim, F. Shokri, A.A. Firoozi, Effect of styrene–butadiene copolymer latex on properties and durability of road base stabilized with Portland cement additive, Constr. Build. Mater. 68 (2014) 740–749.
[36] D. Xuan, A.A. Molenaar, L.J. Houben, Compressive and indirect tensile strengths of cement-treated mix granulates with recycled masonry and concrete aggregates, J. Mater. Civ. Eng. 24 (5) (2011) 577–585.
[37] W.J. Kenis, Predictive design procedures, VESYS Users Manual-An Interim Design Method for Flexible Pavements Using the VESYS Structural Subsystem, U.S. Department of Transportation, Offices of Research & Development, Washington, D.C. 20590: FHWA-RD-77-154, Federal Highway Administration, 1978.
[38] C. Valkering, D. Lancon, E. Dehilster, D. Stoker, Rutting resistance of asphalt mixes containing non-conventional and polymer-modified binders (with discussion and closure), J. Assoc. Asphalt Paving Technol. 59 (1990) 590–609.
[39] K. Kaloush, M. Witczak, Tertiary flow characteristics of asphalt mixtures (with discussion and closure), J. Assoc. Asphalt Paving Technol. 71 (2002) 248–280.
[40] C.L. Monismith, N. Ogawa, C. Freeme, Permanent deformation characteristics of subgrade soils due to repeated loading, Trans. Res. Rec. 537 (1975) 1–17.
[41] P.V. Lade, C. Liggio, J.A. Yamamuro, Effects of non-plastic fines on minimum and maximum void ratios of sand, ASTM Geotech. Test. J. 21 (4) (1998) 336–347.
[42] D.X. Xuan, L.J.M. Houben, A.A.A. Molenaar, Z.H. Shui, Mechanical properties of cement-treated aggregate material – a review, Mater. Des. 33 (2012) 496–502.
[43] J.S. Tingle, J.K. Newman, S.L. Larson, C.A. Weiss, J.F. Rushing, Stabilization mechanisms of nontraditional additives, Trans. Res. Rec.: J. Trans. Res. Board 1989 (1) (2007) 59–67.
[44] A. Molenaar, Design of Flexible Pavement, Lecture Note CT 4860 Structural Pavement Design, Delft University of Technology, The Netherlands, 2007.
[45] P.T. Sherwood, Soil Stabilization with Cement and Lime, Transport Research Laboratory, Department of Transport, London, 1993.
[46] K. Hazirbaba, H. Gullu, California Bearing Ratio improvement and freeze–thaw performance of fine-grained soils treated with geofiber and synthetic fluid, Cold Regions Sci. Technol. 63 (1–2) (2010) 50–60.
[47] A. Maher, W.M. Szalaj, T. Bennert, Evaluation of Poisson's ratio for use in the mechanistic empirical pavement design guide (MEPDG), Division of Research and Technology, Rutgers University, Center for Advanced Infrastructure & Transportation, United States, Federal Highway Administration: Department of Transportation, 2008.
[48] S. Lim, D.G. Zollinger, Estimation of the compressive strength and modulus of elasticity of cement-treated aggregate base materials, Trans. Res. Rec.: J. Transp. Res. Board 1837 (1) (2003) 30–38.
[49] R.L. Terrel, J.A. Epps, E. Barenberg, J. Mitchell, M. Thompson, Soil Stabilization in Pavement Structures, a User's Manual Volume 1: Pavement Design and Construction Considerations, Federal Highway Administration, Department of Transportation, Washington DC, 1979.
[50] AASHTO, Guide for Mechanistic-Empirical Design of New and Rehabilitated Pavement Structures, Final Report prepared for National Cooperative Highway Research Program (NCHRP) 1-37A, National Research Council, Washington DC, 2004.
[51] NCHRP, Characterization of Cementitiously Stabilized Layers for Use in Pavement Design and Analysis, National Cooperative Highway Research Program, Transportation Research Board, Washington State University, Pullman, 2013, pp. 04–36.
[52] A. Ebrahim Abu El-Maaty Behiry, Utilization of cement treated recycled concrete aggregates as base or subbase layer in Egypt, Ain Shams Eng. J. 4 (4) (2013) 661–673.
[53] T. Scullion, J. Uzan, S. Hilbrich, P. Chen, Thickness Design Systems for Pavements Containing Soil Cement Bases, PCA R&D Serial 2863, Portland Cement Association, 2008.
[54] K. Majidzadeh, M. Aly, F. Bayomy, A. El-Laithy, Implementation of a Pavement Design System, Vol. 1 and 2.: EES 578, The Ohio State Univ. Engineering Experiment Station, Columbus, Ohio, 1980.
[55] K.-H. Tseng, R.L. Lytton, Prediction of permanent deformation in flexible pavement materials, Trans. Res. Rec.: J. Trans. Res. Board (1989) 154–172.
[56] R.L. Lytton, J. Uzan, E.G. Fernando, R. Roque, D. Hiltunen, S.M. Stoffels, Development and Validation of Performance Prediction Models and Specifications for Asphalt Binders and Paving Mixes, Strategic Highway Research Program, National Research Council, Washington, D.C., 1993.
[57] M.W. Witczak, Simple performance test for superpave mix design, in: National Cooperative Highway Research Program, National Research Council (U.S.), Transportation Research Board, American Association of State Highway and Transportation Officials, 2002.
[58] T. Baghaee Moghaddam, M. Soltani, M.R. Karim, Evaluation of permanent deformation characteristics of unmodified and polyethylene terephthalate modified asphalt mixtures using dynamic creep test, Mater. Des. 53 (2014) 317–324.
[59] F. Zhou, T. Scullion, L. Sun, Verification and modeling of three-stage permanent deformation behavior of asphalt mixes, J. Trans. Eng. 130 (4) (2004) 486–494.
[60] R.C. West, J. Zhang, J. Allen Cooley, Evaluation of the Asphalt Pavement Analyzer for Moisture Sensitivity Testing, NCAT Report 04-04, National Center for Asphalt Technology, Auburn University, Alabama, 2004.
[61] A. Khodaii, A. Mehrara, Evaluation of permanent deformation of unmodified and SBS modified asphalt mixtures using dynamic creep test, Constr. Build. Mater. 23 (7) (2009) 2586–2592.
[62] A. Wayne, State-of-the-art report on soil-cement, ACI Mater. J.: ACI Committee (1997).
[63] D.T. Davidson, Soil Stabilization with Portland Cement, Highway Research Board Bulletin, National Academy of Sciences, Washington, DC, USA, 1961.
[64] D.N. Little, S. Nair, Recommended Practice for Stabilization of Subgrade Soils and Base Materials, Texas Transportation Institute, National Cooperative Highway Research Program, Transportation Research Board of the National Academies, Texas, US, 2009.
[65] UFC 3-250-11, Soil stabilization for pavements, Departments of the Army the Navy and the Air Force, US: Unified Facilities Criteria (UFC), 2004.
[66] DFID, Literature review: stabilised sub-bases for heavily trafficked roads, Department for International Development, The Transport Research Laboratory, UK, 2003.

[67] K. Gaspard, Evaluation of Cement Treated Base Courses, Louisiana Transportation Research Center, Louisiana Department of Transportation and Development, Louisiana, USA, 2000.
[68] SAPEM, South African Pavement Engineering Manual, South African National Roads Agency Ltd, South African, 2009.
[69] BS 1924, Stabilized materials for civil engineering purposes, General Requirements, Sampling, Sample Preparation and Tests on Materials Before Stabilization, British Standards Institution, London, UK, 1990.
[70] MRTS08.1, Plant-Mixed Stabilised Pavements using Cement or Cementitious Blends, Department of Transport and Main Roads Technical Standard, Australia, 2010.
[71] A.A. Molenaar, D. Xuan, L.J. Houben, Z. Shui, Prediction of the mechanical characteristics of cement treated demolition waste for road bases and subbases, in: Proceedings of the 10th Conference on Asphalt Pavements for Southern Africa, KwaZulu-Natal, South Africa, 2011.
[72] JTJ, Technical specifications for construction of highway roadbases, Ministry of Communications of the People's Republic of China, Beijing, China, Ministry of Communications of the People's Republic of China, 2000.
[73] CCANZ, Cement Stabilisation. Cement & Concrete Association of New Zealand, New Zealand: Cement & Concrete Association of New Zealand, 2008.
[74] AASHTO, Guide for Design of Pavement Structures, American Association of State Highway and Transportation Officials, Washington, D.C., USA, 1993.